Fabrication of a Material Assembly of Silver Nanoparticles Using the Phase Gradients of Optical Tweezers

Zijie Yan, Manas Sajjan, and Norbert F. Scherer

Using Optical Phase Gradients to Assemble Optical Matter from Silver Nanoparticles

Zijie Yan, Manas Sajjan, and Norbert F. Scherer[*]

The James Franck Institute and Department of Chemistry,

The University of Chicago, 929 East 57th Street, Chicago, Illinois 60637, United States

Optical matter can be created using the intensity gradient and electrodynamic (e.g., optical binding) forces that nano- and micro-particles experience in focused optical beams. Here we show that the force associated with phase gradient is also important. In fact, in optical line traps the phase gradient force is crucial in determining the structure and stability of optical matter arrays consisting of Ag nanoparticles (NPs). NP lattices can be repeatedly assembled and disassembled simply by changing the sign of the phase gradient. The phase gradient force induces strain in optically bound Ag NP lattices, causing structural transitions from 1-D "chains" to 2-D lattices, and even to amorphous structures. The structural transitions and dynamics of driven transport are well described by electrodynamics simulations and a drift-diffusion Langevin equation.

Optical matter, ordered assemblies of small particles drawn together and stabilized by electrodynamic inter-particle forces in an optical field, represents a unique type of material [1]. Since the first observation of optical binding between two dielectric microparticles by Burns et al. [2], theoretical and experimental investigations of optical binding have significantly enriched the examples of optical matter [3-12]. Notably, Grzegorczyk et al. [13] recently made a major step toward laser-trapped mirrors [14] by assembling a monolayer of ~150 optically bound polystyrene microspheres at a dielectric surface in water. Assembling such an extended optical matter system is challenging. One needs a spatially extended optical beam to illuminate the particles with sufficient intensity to overcome Brownian random forces. Both the gradient forces that confine the (individual) particles, and the optical binding forces that can unite the particles into arrays, are linearly proportional to the intensity. Apart from increasing the laser power to enhance optical binding, metal NPs provide an alternative solution for creating large scale optical matter assemblies. Metal NPs exhibit much stronger light scattering, per unit volume, compared to dielectric particles, leading to "ultra-strong" optical binding forces [15]. The structure of optically bound metal NPs can be controlled by adjusting the intensity gradient of the trapping beam [16]. If other optical

forces could be added to the well-known optical binding and gradient forces one could have greater control over the dynamics of assembly and structures formed.

In this letter, we demonstrate that the *phase gradient* of an extended optical field can strongly affect the self-organization of optical matter. The phase gradient has generally been ignored in optical trapping; most typically the optical force transverse to the optical axis of a linearly polarized laser beam is assumed to be solely due to the intensity gradient, i.e., the "gradient force" [4,17]. However, recently Grier and colleagues demonstrated that strong optical forces could also arise from phase gradients in an extended beam of light by redirecting radiation pressure to the transverse plane [18]. Here we show that phase-gradient forces drive assembly and allow tailoring the structures of Ag NP arrays in optical line traps. Optical line traps have been used for studying optical binding [2,11,12,15,19]. A typical optical line provides a strongly focused field along the short axis to confine the particles (in 1-D) yet a relatively flat intensity profile along the long axis that facilitates optical binding interactions over many particles. Interestingly, the 1-D lattices of optical matter that we create can exhibit structural instabilities associated with a yield stress. In particular, we show that a structural collapse occurs in the central portion of larger Ag NP arrays, even with a flat intensity profile. Our electrodynamics simulations reveal that the structural changes arise from a compressive phase gradient force that is extensive in the number of NPs.
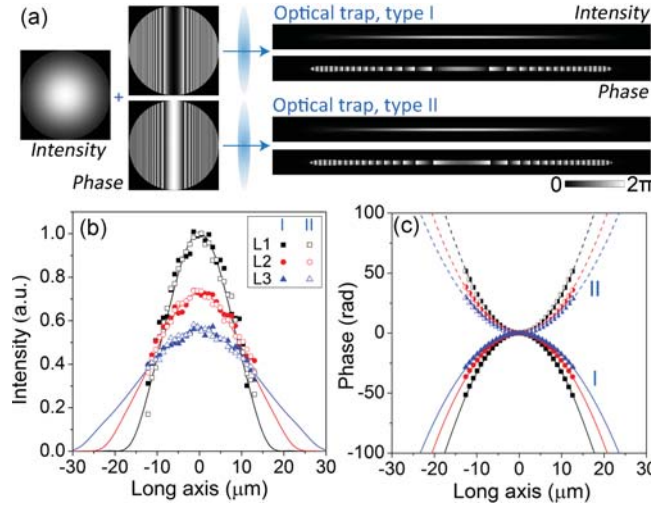

FIG. 1. (a) Generation of optical line traps by phase modulation of a Gaussian beam. Left: images of the incident beam profile and complementary phase masks used in the experiments. Right: images of the intensity (top) and phase (bottom) profiles predicted from the Fourier transforms of the phase masks as performed by the objective lens. (b) The intensity profiles and (c) the phase profiles along the long axes of the line traps measured using a wavefront sensor. The measured results for three different profiles (L1 L3) are shown as filled and open points (type I and II, respectively). The solid and dashed lines are the corresponding profiles calculated from the incident beam and phase masks for type I and type II phase profiles on the SLM.

We begin by demonstrating that the phase gradient, rather than intensity gradient, strongly influences the dynamics of single Ag NPs in aqueous solution confined by an optical line trap over a coverslip. Citrate coated Ag NPs with diameters of 151±13 nm were used in the experiments, and optical line traps were created by phase modulation of a collimated Gaussian beam ($\lambda = 800$ nm in vacuum) using a spatial light modulator (Fig. 1(a), also see section I in the Supplemental Material [20]). To distinguish the contributions of phase and intensity gradients to the total optical force on a NP, we designed two types of optical line traps; they have the same intensity profile but opposite phase gradients (denoted as type I and type II). The phase mask for a type I optical trap represents the phase modulation caused by a convex cylindrical lens while that for a type II trap represents the phase modulation by a concave cylindrical lens. They generate the same intensity distribution at the focal plane of a spherical lens (Fig. 1(a) and lines in Fig. 1(b)), but exactly opposite phases along the long axis of the optical lines (Fig. 1(a) and lines in Fig. 1(c)). In the experiments, we produced three pairs of line traps (each with two types of phase profiles); denoted as L1, L2 and L3 with increasing lengths and thus decreasing maximum intensities. We measured their intensity and phase profiles using an optical wavefront sensor (Fig. S1 [20]). The measured profiles (data points in Fig. 1(b) and 1(c)) agree well with the target parabolic profiles (solid and dashed lines) that we designed.
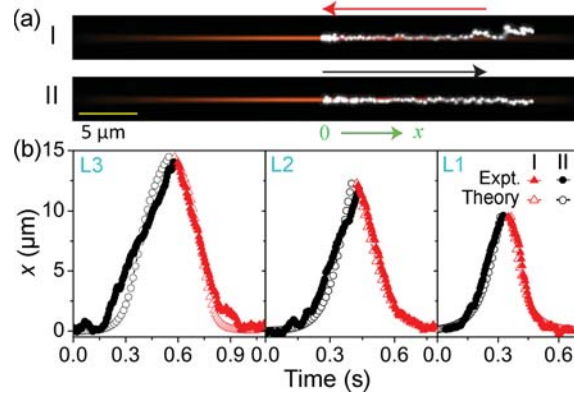

FIG. 2. (a) Trajectories of a single Ag NP (150 nm diameter) in two different types of line traps. The white dots are darkfield optical images of the Ag NP obtained with a frame rate of 200 fps that are superimposed on the images of the line traps (red). The calculated intensity profiles of the line traps (pair L2) are shown in red for reference. $x = 0$ indicates the center of a trap. (b) Representative motions (trajectories) of single Ag NPs in line traps with different intensity and phase profiles. Note that each segment of the trajectories (i.e., the black and red parts) represents the motion of a single Ag NP in a type II then type I phase profile. The maximum distance to the center in each panel corresponds to a position where the line trap could confine the NPs along its short axis. The lateral trapping forces become weak

close to the ends of the traps; see Fig. S3 [20]. Theoretical trajectories calculated using a Langevin equation model are also shown for comparison.

Using these pairs of line traps, it is possible to determine the relative magnitudes of the intensity-gradient force (F_{int}) and the phase-gradient force (F_{pha}) exerted on a single Ag NP. Note that $F_{int} \propto \nabla I$ and $F_{pha} \propto I \nabla \varphi$ [18,28], where I and φ correspond to the intensity and phase of the field, respectively. For a Gaussian intensity profile and a parabolic phase profile, $F_{int} = C_1 x \exp(-x^2 / w^2)$ and $F_{pha} = C_2 x \exp(-x^2 / w^2)$ where C_1 and C_2 are constants and w is a scale parameter of the Gaussian intensity profile (see sections II and VIII in [20]). F_{int} always tends to attract a NP to the center of a line trap, while F_{pha} does the same in a type I line trap (i.e., $C_1 < 0$), but repels the NP towards the distal ends in a type II line trap (i.e., $C_2 > 0$). As a result, a comparison of the directions of motion of a NP establishes the dominant force. Fig. 2 clearly shows that a single NP moves from either end to the center of a type I line trap, and moves from the center to either end in a type II trap.

With the coordinates of Fig. 2(a), the total optical force for a type I trap is

$$F_I = -\left|F_{int}\right| - \left|F_{pha}\right| = A_1 x \exp(-x^2 / w^2), \qquad (1)$$

and the total optical force for a type II trap is

$$F_{II} = -\left|F_{int}\right| + \left|F_{pha}\right| = A_2 x \exp(-x^2 / w^2), \qquad (2)$$

where constants $A_1 < 0$ and $A_2 > 0$. In this sign convention we assume a force that drives a NP to the center of a trap to be negative. Assuming a uniform rectilinear motion of a Ag NP in a Stokes flow, and from the fluctuation-dissipation relation [29], the total optical force would be $F_{opt} = F_d$ where $F_d = 6\pi\mu R v$ is the viscous drag force, μ is the dynamic viscosity of water, R is the hydrodynamic radius of the NP, and v is the particle's velocity. The velocities are estimated by fitting the NP trajectories (e.g., the portions of distances > 1.5 μm in the experimental trajectories of Fig. 2(b)) with linear functions; the velocities are given by the slopes. The results are shown in Fig. S4 [20] and the calculated optical forces $|F_{pha}|$ and $|F_{int}|$ are summarized in Table 1 assuming NP heating (the estimated temperature increase at the NP surface is 21 K; see section V in [20]). It is clear that the phase-gradient forces are much larger than the intensity-gradient forces, demonstrating that the phase gradients rather than the intensity gradients determine the dynamics of NPs confined by optical line traps. This conclusion is also applicable for much smaller Ag NPs (e.g., 40 nm dia.), and is supported by our Finite-difference time-domain (FDTD) simulations presented in section VI of [20].

4

Table 1. Optical forces calculated using Stokes' law.

Pair of traps	$|F_{pha}|$ (fN)	$|F_{int}|$ (fN)
L1	56	7
L2	46	6
L3	34	5

The dynamics of a single Ag NP in the field of the optical forces are described using a 1D-generalized Langevin equation:

$$\ddot{q} = \frac{F(q)}{m} - \int_0^t \xi(t-\tau)\dot{q}(\tau)\,d\tau + \frac{\eta(t)}{m}, \qquad (3)$$

where m is the mass of the particle, q is the generalized displacement coordinate for the NP, $F(q)$ corresponds to the total optical force experimentally simulated in the medium (i.e., Eqs. 1 & 2), $\xi(t-\tau)$ corresponds to the dissipative memory kernel and $\eta(t)$ is the Gaussian random noise. This equation can be simplified to [20]:

$$\gamma\langle\dot{q}\rangle = F(q), \qquad (4)$$

where γ is the frictional coefficient between the NP and the medium. The simulated single NP trajectories agree well with the experimental data (Fig. 2(b)); parameters for the simulation are presented in Table 2.

Table 2. Parameters of the Langevin model used for simulating the single NP dynamics in optical lines.

Pair of traps	A_1 (fN)	A_2 (fN)	w (μm)	γ (fNs/μm)
L1	27	-30	9.2	
L2	21	-22	13.0	1.31
L3	18	-19	17.0	

When multiple Ag NPs are confined by a line trap, optical binding forces arising from the electrodynamic interactions among these NPs lead to the formation of arrays of regularly spaced structures, i.e., optical matter. In theory, the optical matter in a quasi-1-dimensional field will be single linear chain of NPs separated by distances (approximately) equal to an integral number of wavelengths of light in the medium [3,11]. Such optical binding behavior is clearly exhibited by the trajectories and images of 5–8 Ag NPs in Fig. 3(a) (i.e., from 0 to 1 s). However, when there are 10 or more Ag NPs in the chain, the optical matter undergoes structural changes for the present experimental conditions. In particular, dimers aligned along the short axis spontaneously form near the chain's center. Two structural change events are shown in the optical images in Fig. 3(b) where a NP moves alongside its neighbor in

the *x-y* plane (the beam propagates along the *z*-direction), resulting in a dimer along the short axis. Similar structural changes are shown in Fig. S5 [20].

Fig. 3(c) shows that the linear chains of optical matter exhibit instabilities and undergo transitions between crystalline and amorphous structures when there are many Ag NPs, for example ≥ 20 NPs in the trap. Interesting metastable lattices appear, e.g., at 385 ms and 1785 ms. These results indicate that as the NP chain gets longer, the force from the interacting particles in the optical line trap becomes large and eventually overwhelms the optical binding interactions [16]. We denote the structural changes a "phase transition"; from 1-D chains to 2-D arrays to dynamic amorphous structures.
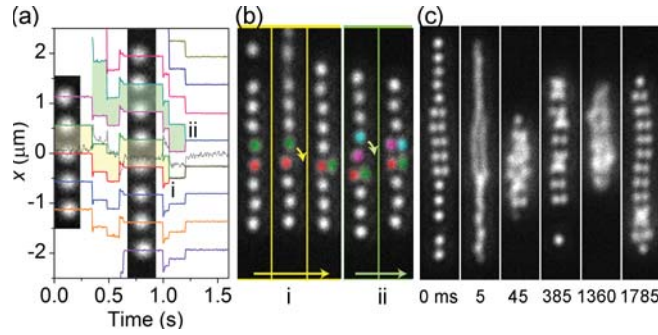

FIG. 3. (a) Trajectories of Ag NPs self-organizing in a type I (i.e. compressive) line trap. The solid lines are the centroid positions of the NPs relative to the center-of-mass (the black dashed line) of the whole chain. Note that two trajectories (i.e., the top and bottom boundary lines of the yellow and cyan shaded regions) merge into a single line at times i and ii, respectively, indicating dimer formation events. (b) Representative darkfield images of NPs undergoing structure evolution (the time interval between the panels is 5 ms) corresponding to the two events in panel a. NPs of interest are marked with artificial colors. (c) Images of another chain that exhibits rapid transitions between crystalline, metastable and amorphous structures.

When multiple Ag NPs self-organize in a type I optical line trap, the phase gradient exerts a centrosymmetric compressive optical force on the NP chain. This compressive force causes the central region of the chain to behave as a rigid body [11,12]. The center-of-mass of the chain tends to be coincident with the center of the trap as indicated by the dashed line in Fig. 3(a). Our FDTD simulation (section VII of [20]) reveals that this compression can induce structural changes when the length of the NP chain exceeds a threshold. As shown in Fig. 4(a) and (b), a chain of 11 (or fewer) NPs can self-organize into a stable linear structure in a simulated line trap that is similar to our experimental conditions. However, the structure collapses for 12 (or more) NPs, typically at the central pair. The collapse is triggered by the continuous inward translation of the terminal NPs and their addition to the

total inward force. Thus, more axial force (stress) is exerted on the central pair of NPs when more particles are in the line trap.

This structural instability is not an intrinsic property of optical binding when one assumes a plane wave optical field. To make this clear, we also investigated the self-organization of NP chains in a plane wave. The results show that long chains are stable (curves 1&2 in Fig. 4(b) and Fig. S11 [20]), and the separations of adjacent NPs in a plane wave are always larger than those in an optical line trap (curves 3&4), indicating weaker compression by optical forces in the plane wave. In fact, Fig. 4(b) shows that the chain *tends to expand with more NPs in the plane wave*, but this trend is only maintained for a few NPs (e.g., ≤ 6) in the optical line. This observation shows that there is a threshold where the axially compressive optical force becomes comparable or even larger than the optical binding force and eventually causes collapse of the central pair. In principle, the near-field electrodynamic interaction would result in the particles forming an aggregate, but this is prevented by Coulomb repulsion since the Ag NPs are coated with charged surfactants to prevent aggregation. So, when the inter-particle separation decreases significantly, the Coulomb repulsion and near-field electrodynamics interactions generate forces that tend to rotate the pair to the light polarization direction as shown in Fig. 4(c). Therefore, as shown in Fig. 3(b), dimers perpendicular to the long axis will form in long chains and do so until the stress is reduced below a critical value.
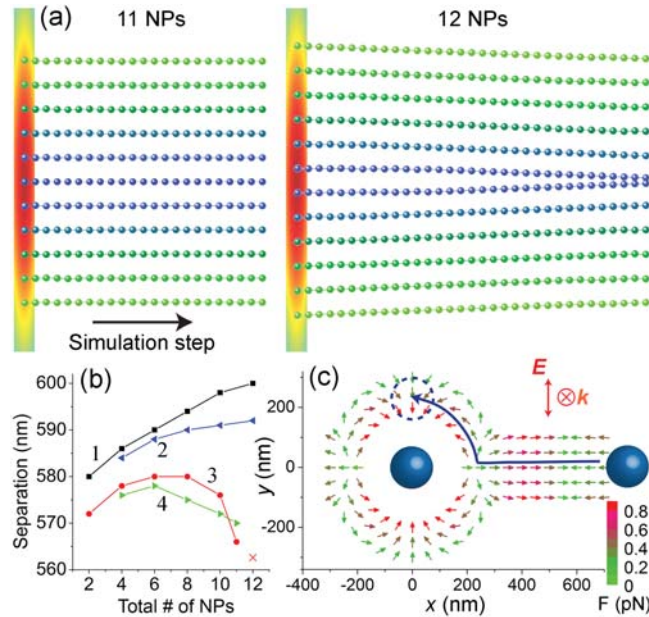

FIG. 4. (a) FDTD simulation of the structural change (stabilization or collapse) of Ag NPs in a type I line trap. (b) Equilibrium separations between adjacent NP pairs in the central region (curves 1,3) and at the termini (curves 2,4). Plane wave (curves 1,2) as well as the line trap (curves 3,4) are used in the simulation. (c) Optical forces between a pair of Ag NP in the central region of the line trap. (d) Optical

forces on a Ag NP when it is located near the central region of a chain with 10 NPs in the line trap. The black dashed circle indicates the trapping positions of the NP. The solid blue curve shows a possible path for structural collapse where the inter-particle separation along the chain axis (*x*-axis) is reduced and the particle shifts to the transverse orientation (along the *y*-axis).

We also observed another dimer formation mechanism where a NP moves along the negative *z*-direction (i.e., out of the focal plane) and gets temporarily trapped between two neighbors before jumping to the side of one of them to form a dimer. This mechanism, which is similar to the co-trapping behavior we reported in [12], is shown and explained in section IV of [20].

These strong axial forces, here primarily from the phase gradients, allow exploring the phase diagram of optical matter. In traditional materials, an external force imposes a stress on a material, which then deforms or undergoes a structural change or even a phase transition in order to relax the strain. For example, the crystalline structures of ice, silica and many other materials become unstable and even amorphous at high pressure due to pressure-induced amorphization [30-32]. The response of Ag NP chains to the optical forces can be viewed in a similar way: the chains tend to form dimers under axially compressive stress in order to relax the strain and attain a new stable structure. However, if the forces are too strong, here because of a large number of particles in the trap, the optical matter accumulates too much stress in both the axial and transverse directions and becomes dynamically amorphous.

In conclusion, we have shown that optical phase gradients can be used to tailor the self-organization of optical matter in an extended optical field. The structures and structural changes we report here make clear the analogy between optical matter and traditional materials, and, more importantly, reflect the fact that a rich phase diagram of the structures of optical matter exists and awaits further exploration. Since it is easy to modify the phase profile of an optical field by a spatial light modulator, it may be possible to design a phase landscape to guide the self-organization of micro/nanoparticles. Understanding and tuning phase-related optical potentials will facilitate the design and fabrication of optical matter for applications such as the "laser-trapped telescope" mirrors [14], and the discovery of materials with novel properties. The insights provided here may thus benefit the research in optics and photonics, astronomy, materials science, and many other fields.

*Corresponding author.

nfschere@uchicago.edu

References:

[1] M. M. Burns, J. M. Fournier, and J. A. Golovchenko, Science **249**, 749 (1990).

[2] M. M. Burns, J. M. Fournier, and J. A. Golovchenko, Phys. Rev. Lett. **63**, 1233 (1989).

[3] K. Dholakia and P. Zemánek, Rev. Mod. Phys. **82**, 1767 (2010).

[4] T. Čižmár, L. C. D. Romero, K. Dholakia, and D. L. Andrews, J. Phys. B: At. Mol. Opt. Phys. **43**, 102001, 102001 (2010).

[5] D. Haefner, S. Sukhov, and A. Dogariu, Phys. Rev. Lett. **103**, 173602 (2009).

[6] V. Karasek, T. Cizmar, O. Brzobohaty, P. Zemanek, V. Garces-Chavez, and K. Dholakia, Phy. Rev. Lett. **101**, 143601, 143601 (2008).

[7] J. Ng, Z. F. Lin, C. T. Chan, and P. Sheng, Phys. Rev. B **72**, 085130 (2005).

[8] J. Rodriguez, L. C. Davila Romero, and D. L. Andrews, Phys. Rev. A **78**, 043805, 043805 (2008).

[9] C. D. Mellor, T. A. Fennerty, and C. D. Bain, Opt. Express **14**, 10079 (2006).

[10] Z. P. Li, M. Kall, and H. Xu, Phys. Rev. B **77**, 085412, 085412 (2008).

[11] Z. Yan, R. A. Shah, G. Chado, S. K. Gray, M. Pelton, and N. F. Scherer, ACS Nano **7**, 1790 (2013).

[12] Z. Yan, U. Manna, W. Qin, A. Camire, P. Guyot-Sionnest, and N. F. Scherer, J. Phys. Chem. Lett. **4**, 2630 (2013).

[13] T. M. Grzegorczyk, J. Rohner, and J.-M. Fournier, Phys. Rev. Lett. **112**, 023902 (2014).

[14] A. Labeyrie, Astron. Astrophys. **77**, L1 (1979).

[15] V. Demergis and E.-L. Florin, Nano Lett. **12**, 5756 (2012).

[16] Z. Yan, S. K. Gray, and N. F. Scherer, Nat. Commun. **5**, 3751 (2014).

[17] O. M. Marago, P. H. Jones, P. G. Gucciardi, G. Volpe, and A. C. Ferrari, Nat. Nanotech. **8**, 807 (2013).

[18] Y. Roichman, B. Sun, Y. Roichman, J. Amato-Grill, and D. G. Grier, Phys. Rev. Lett. **100**, 013602 (2008).

[19] Z. Yan, Y. Bao, U. Manna, R. A. Shah, and N. F. Scherer, Nano Lett. **14**, 2436 (2014).

[20] See Supplemental Material at http://link.aps.org/supplemental, which includes Refs. [21-27], for I. Methods, II. Optical line profiles and forces, III. NP motion, trajectories, and speeds, IV. Structures of optically bound NP arrays, V. Heating of NPs in the optical line, VI. Optical forces on smaller NPs, VII. Electrodynamics simulation, and VIII. Langevin dynamics simulation.

[21] https://www.lumerical.com/tcad-products/fdtd/.

[22] P. B. Johnson and R. W. Christy, Phys. Rev. B **6**, 4370 (1972).

[23]   G. Baffou, R. Quidant, and F. J. García de Abajo, Acs Nano **4**, 709 (2010).

[24]   K. C. Neuman and S. M. Block, Rev. Sci. Instrum. **75**, 2787 (2004).

[25]   M. Dienerowitz, M. Mazilu, and K. Dholakia, J. Nanophoton. **2**, 021875 (2008).

[26]   W. T. Coffey and Y. P. Kalmykov, *The Langevin Equation: With Applications to Stochastic Problems in Physics, Chemistry and Electrical Engineering* (World Scientific, 2012), World Scientific Series in Contemporary Chemical Physics.

[27]   U. M. B. Marconi, A. Puglisi, L. Rondoni, and A. Vulpiani, Phys. Rep. **461**, 111 (2008).

[28]   D. B. Ruffner and D. G. Grier, Phys. Rev. Lett. **111**, 059301 (2013).

[29]   R. Zwanzig, *Nonequilibrium Statistical Mechanics* (Oxford University Press, 2001).

[30]   O. Mishima, L. D. Calvert, and E. Whalley, Nature **310**, 393 (1984).

[31]   R. J. Hemley, A. P. Jephcoat, H. K. Mao, L. C. Ming, and M. H. Manghnani, Nature **334**, 52 (1988).

[32]   D. Machon, F. Meersman, M. C. Wilding, M. Wilson, and P. F. McMillan, Prog. Mater. Sci. **61**, 216 (2014).